

SUPPLEMENTARY INFORMATION

Effective Fluoride Removal Using Granular Bauxite Filter Media as an Affordable and Sustainable Alternative to Activated Alumina

Katya Cherukumilli^{a*}, Max Steiner^b, Jessica R. Ray^a

^a Department of Civil and Environmental Engineering, University of Washington, Seattle, WA, 98195, USA

^b Department of Chemical Engineering, University of Washington, Seattle, WA, 98195, USA

*** Corresponding Author.** Katya Cherukumilli, E-mail: katyacherukumilli@gmail.com

Table of Contents	Page No.
1. Synthetic Groundwater Recipe	2
2. Control Columns (100 wt.% Sand) Data - Fig. S1	2
3. Experimental Setup of Filter Column - Fig. S2	3
4. Effect of Activated Alumina Particle Size on Adsorption Kinetics - Fig. S3	4
5. Effect of Synthetic Groundwater Initial pH on Adsorption Kinetics - Fig. S4	5
6. Weber and Morris Intraparticle Diffusion Model - Fig. S5	6
7. Effect of Kinetics and Solution Matrix on Metal Dissolution – Fig. S6	7
8. Effect of Adsorbent Dose on Metal Dissolution – Fig. S7	8
9. Freundlich Adsorption Isotherm Model - Fig. S8	9
10. Filter Column Breakthrough by Number of Pore Volumes - Fig. S9	10
11. Parameter Value Estimation for BDST Model - Fig. S10	11
12. Estimation of Time to Filter Media Saturation	12
13. Fluoride Adsorption Kinetics Normalized by Particle Size - Fig. S11	13

1. Synthetic Groundwater Recipe

To minimize the precipitation of solids, synthetic groundwater (SGW) was prepared by adding stock solutions in this sequence: Milli-Q deionized water, anionic salts (NaHCO_3 , NaNO_3 , Na_2SO_4 , NaF), and cationic salts ($\text{CaCl}_2 \cdot 2\text{H}_2\text{O}$, $\text{MgCl}_2 \cdot 6\text{H}_2\text{O}$). The concentrations of electrolytes (Na^+ , K^+ , Cl^-) present in the added salts were within 1 mM of the median values in the SGW recipe. All chemicals used to prepare solutions in this study were ACS reagent grade. Calcium chloride dihydrate ($\text{CaCl}_2 \cdot 2\text{H}_2\text{O}$) was purchased from Sigma Aldrich, sodium bicarbonate and sodium fluoride (NaHCO_3 and NaF) were purchased from Fisher Scientific, and magnesium chloride hexahydrate, sodium chloride, sodium sulfate, and sodium nitrate ($\text{MgCl}_2 \cdot 6\text{H}_2\text{O}$, NaCl , Na_2SO_4 , NaNO_3) were purchased from VWR. The references and raw data used to generate the synthetic groundwater recipe can be accessed in the attached excel file, “Supplemental Data.xlsx”. The raw groundwater composition data was cleaned by converting all reported concentrations to standard units of ppm (mg L^{-1}), removing any water samples with fluoride concentrations below $1.5 \text{ mg F}^- \text{ L}^{-1}$ (WHO limit), and changing any concentrations reported as “ $< 0.1 \text{ mg L}^{-1}$ ”, “Below Detection Limit”, or “ND” to zero.

2. Control Columns (100 wt.% Sand) Data - Fig. S1

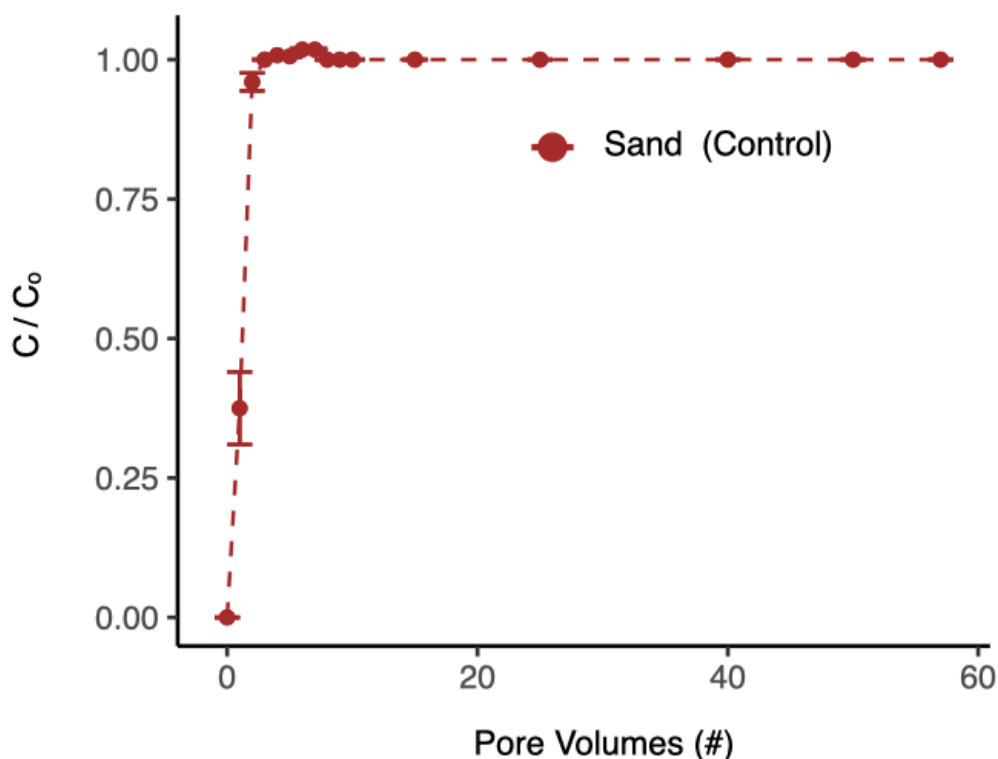


Fig. S1. Fluoride breakthrough ($C_0 = 5 \text{ mg F}^- \text{ L}^{-1}$) in control columns filled with 100 wt. % sand is almost instant. The dashed line connects raw experimental data points. This data suggests negligible fluoride adsorption onto sand and the inert polyester material used in filters columns as a barrier to prevent loss of media. Error bars represent standard errors calculated from duplicate measurements.

3. Experimental Setup of Filter Column - Fig. S2

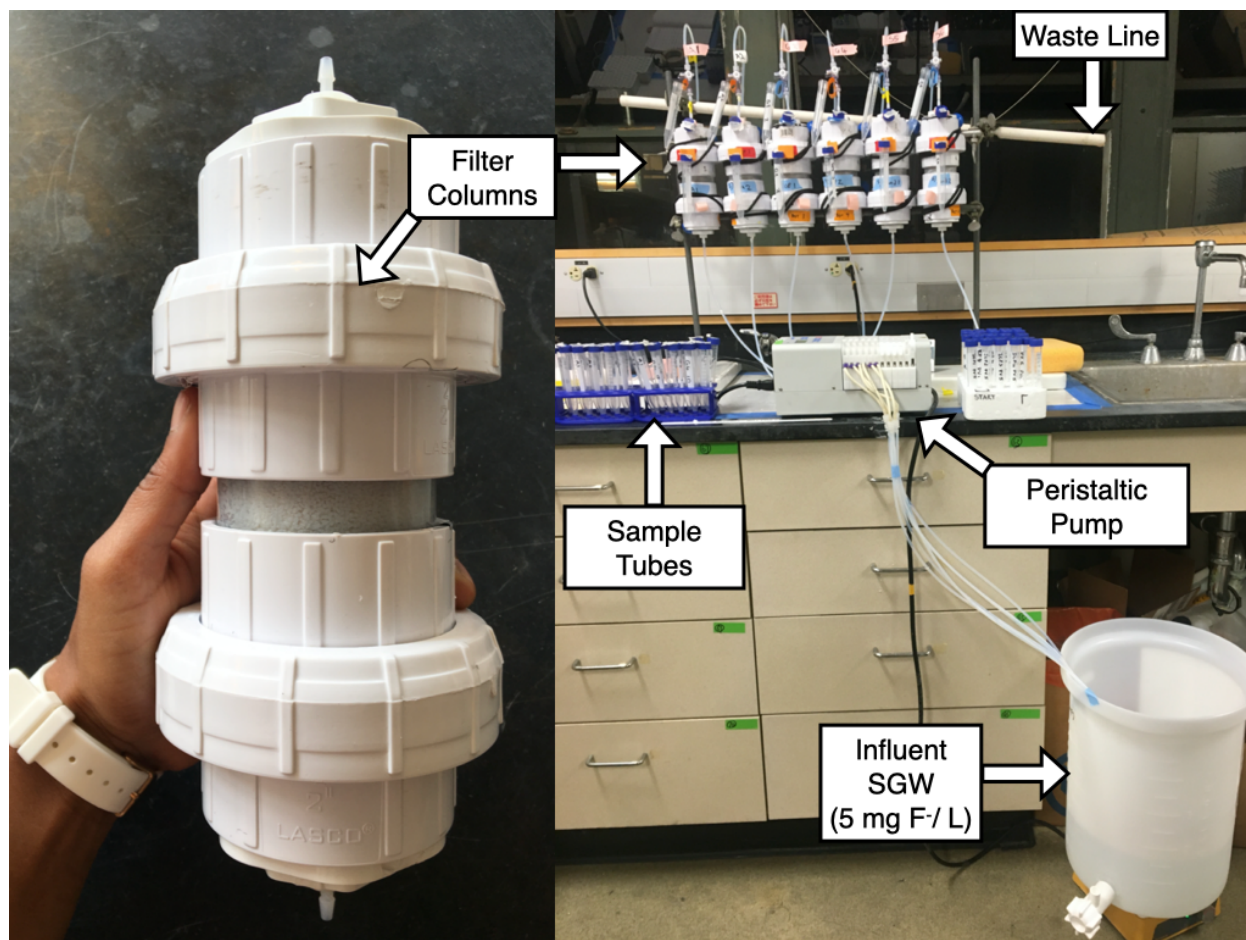


Fig. S2. Small column filters (height = 7.9 cm, ID = 2 inch) were built using materials purchased from McMaster Carr (e.g., PVC pipe, fittings, adapters, union connectors, barbed plugs, and sockets, etc.). Approximately 2 grams of 100% polyester filter floss (Blue Ribbon Pet Products) was packed in either end of each column as a barrier media to prevent media loss. Packed columns were mounted to metal lab stands, connected to tubing purchased from Cole Parmer (Ismatec SC0336 2-Stop, PharMed BPT Tubing, 2.79 mm ID) and McMaster Carr (Extreme-Temperature Teflon® PTFE Semi-Clear Tubing for Chemicals, 1/8 inch ID). An Ismatec IPC 12-channel peristaltic pump was used to control the upward flow rate of water through the columns. Column effluent that was not collected for sampling purposes was directly discharged into a nearby sink, in compliance with University of Washington's environmental health and safety protocols.

4. Effect of Activated Alumina Particle Size on Adsorption Kinetics - Fig. S3

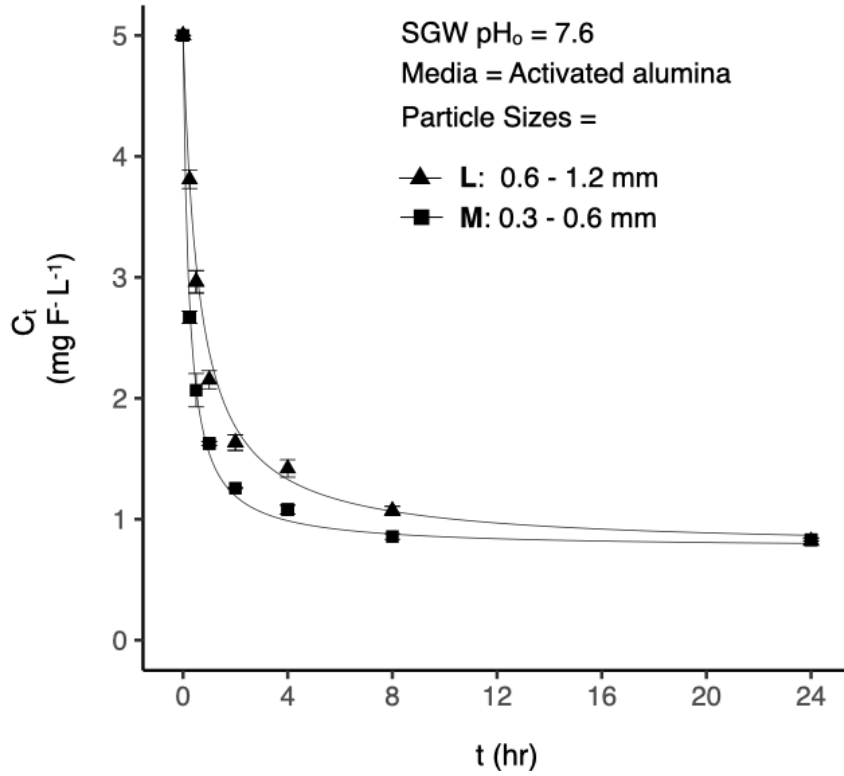


Fig. S3. Kinetics of fluoride adsorption by commercially purchased activated alumina (particle sizes **L**: 0.6-1.2 mm; **M**: 0.3-0.6 mm) modeled by the pseudo-second order (PSO) kinetics rate law (solid lines). All linear regression R^2 correlation coefficients ranged between 0.99-1.0. Batch experiments in synthetic groundwater ($pH_0 = 7.6$) with an initial fluoride concentration of 5 mg $F^- L^{-1}$ and media dose of 8 g L^{-1} . Averages of fluoride concentration measurements taken from triplicate experiments are presented, along with calculated standard deviations.

The pseudo second order (PSO) kinetics rate model proposes that the driving force behind continued adsorption is directly proportional to the fraction of remaining sorption sites available at a given time (Blanchard et al., 1984):

$$\frac{dq_t}{dt} = k_2(q_e - q_t)^2 \quad (S1)$$

Plotting the linearized PSO model allowed for estimation of model parameters including the kinetics rate constant (k_2 in $g\ mg^{-1}\ hr^{-1}$), adsorption density at equilibrium (q_e in $mg\ g^{-1}$), and adsorption density at a given time (q_t , in $mg\ g^{-1}$):

$$\frac{t}{q_t} = \frac{1}{k_2 q_e^2} + \frac{1}{q_e} t \quad (S2)$$

5. Effect of Synthetic Groundwater Initial pH on Adsorption Kinetics - Fig. S4

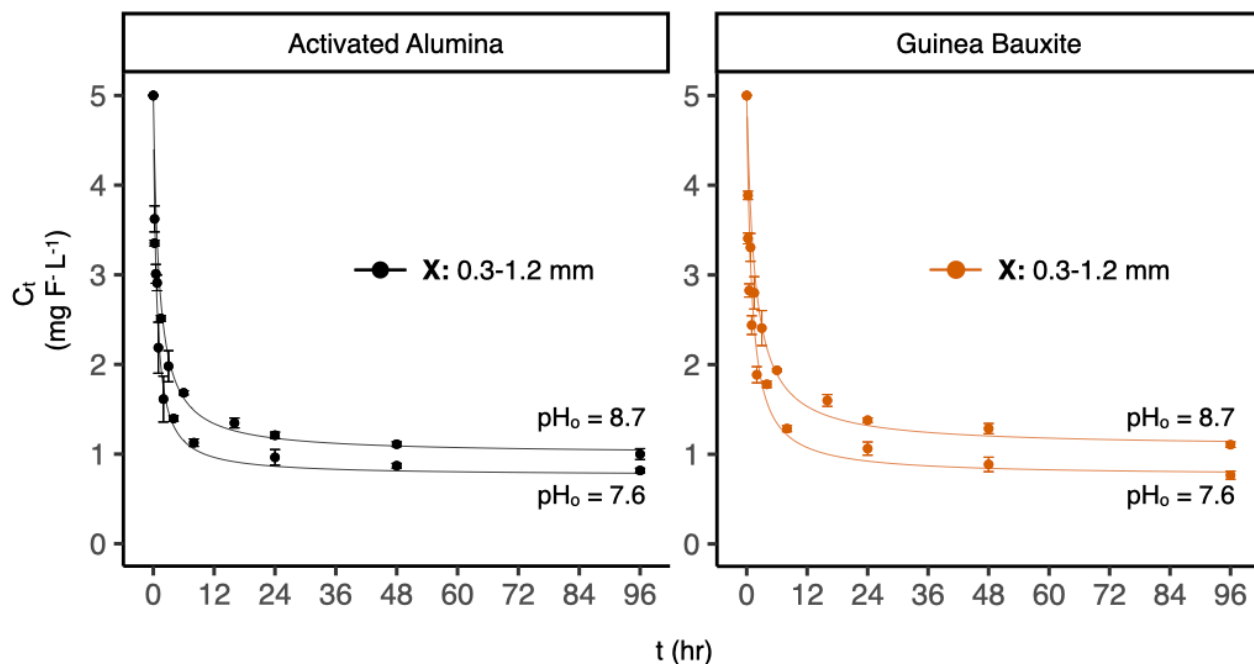


Fig. S4. Kinetics of fluoride adsorption by commercially purchased activated alumina and Guinea bauxite (particle sizes X : 0.3-1.2 mm) modeled by the pseudo-second order (PSO) kinetics rate law (solid lines). Batch experiments in acidified ($pH_o = 7.6$) and unaltered ($pH_o = 8.7$) synthetic groundwater with an initial fluoride concentration of 5 mg F⁻ L⁻¹ and media dose of 8 g L⁻¹. Averages of fluoride concentration measurements taken from triplicate experiments are presented, along with calculated standard deviations.

6. Weber and Morris Intraparticle Diffusion Model - Fig. S5

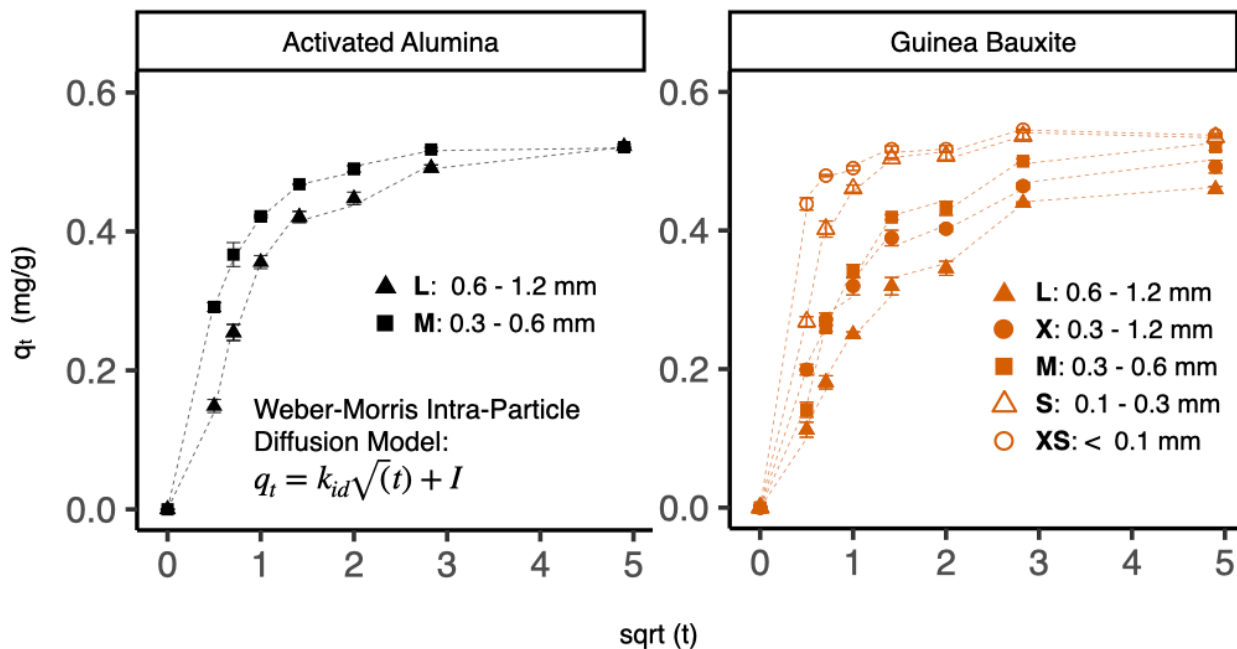


Fig. S5. Weber and Morris models plotted as adsorption density against square root of time for different particle sizes of activated alumina and Guinea bauxite. Dashed lines connect raw experimental data points and are drawn to help guide the eye. The model indicates that a rate-determining step in adsorption up to an adsorption density of approximately $q/q_e = 0.3$ is likely intraparticle diffusion of fluoride through porous structures within activated alumina and Guinea bauxite (especially for larger particle sizes).

7. Effect of Kinetics and Solution Matrix on Metal Dissolution – Fig. S6

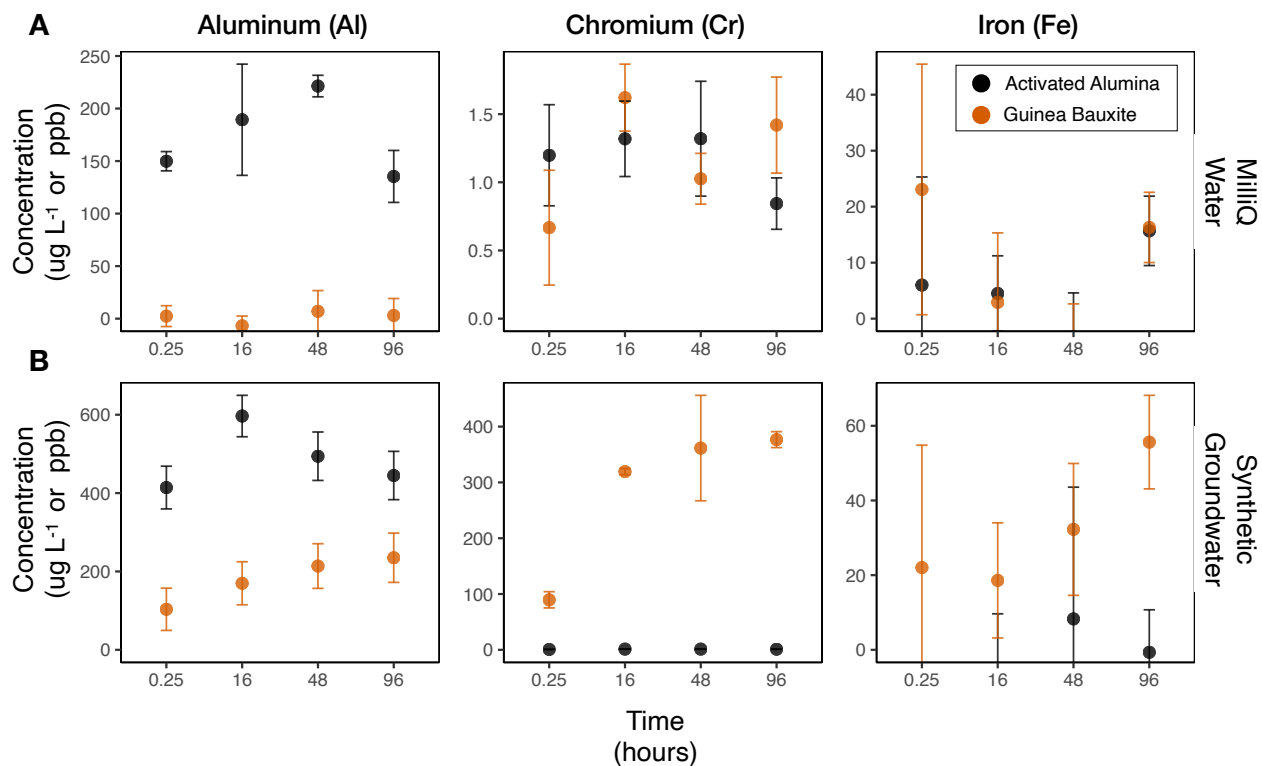


Fig S6. Kinetics of metal dissolution in batch experiments conducted using activated alumina and heated Guinea bauxite (particle size \mathbf{X} : 0.3-1.2 mm; adsorbent dose = 4 g L^{-1}) in: **(A)** Milli-Q water and **(B)** Synthetic groundwater ($\text{pH}_0 = 8.7$; $C_0 = 5 \text{ mg F}^{-} \text{ L}^{-1}$). The US Environmental Protection Agency's drinking water quality standards currently enforce a primary maximum contaminant limit for chromium ($100 \mu\text{g L}^{-1}$ total Cr) and provide recommend limits for aluminum ($200 \mu\text{g L}^{-1}\text{Al}$) and iron ($300 \mu\text{g L}^{-1}\text{Fe}$). Averages of metal concentrations measured in triplicate experiments are presented, along with calculated standard deviations.

8. Effect of Adsorbent Dose on Metal Dissolution – Fig. S7

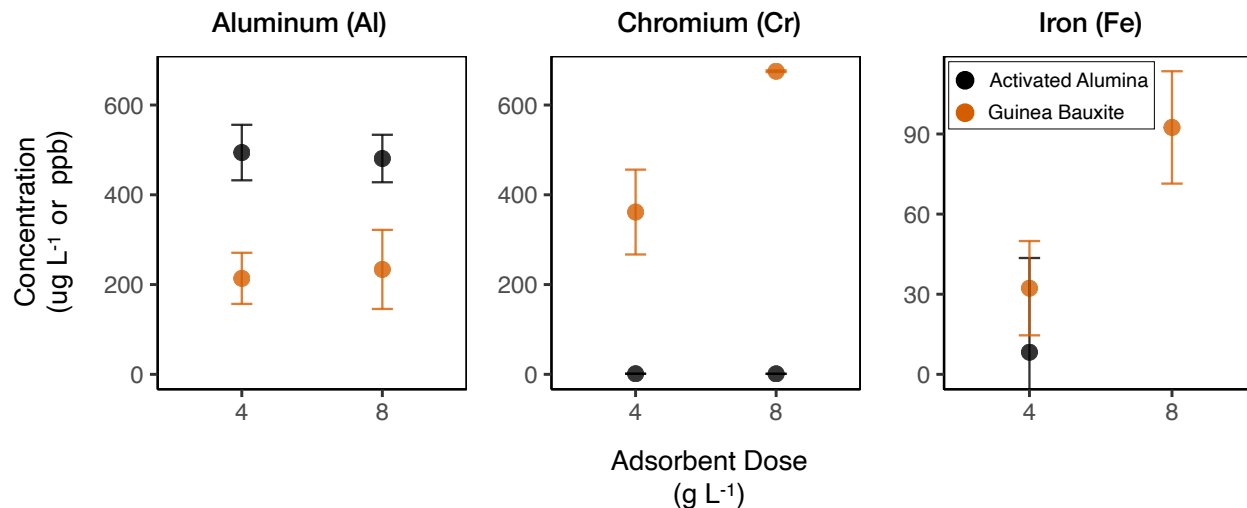


Fig S7. Impact of adsorbent dose (4 or 8 g L⁻¹) on metal dissolution in 48-hr batch experiments conducted using activated alumina and heated Guinea bauxite (particle size **X**: 0.3-1.2 mm) in a synthetic groundwater matrix (pH₀ = 8.7; C₀ = 5 mg F⁻ L⁻¹). Averages of metal concentrations measured in triplicate experiments are presented, along with calculated standard deviations.

9. Freundlich Adsorption Isotherm Model - Fig. S8

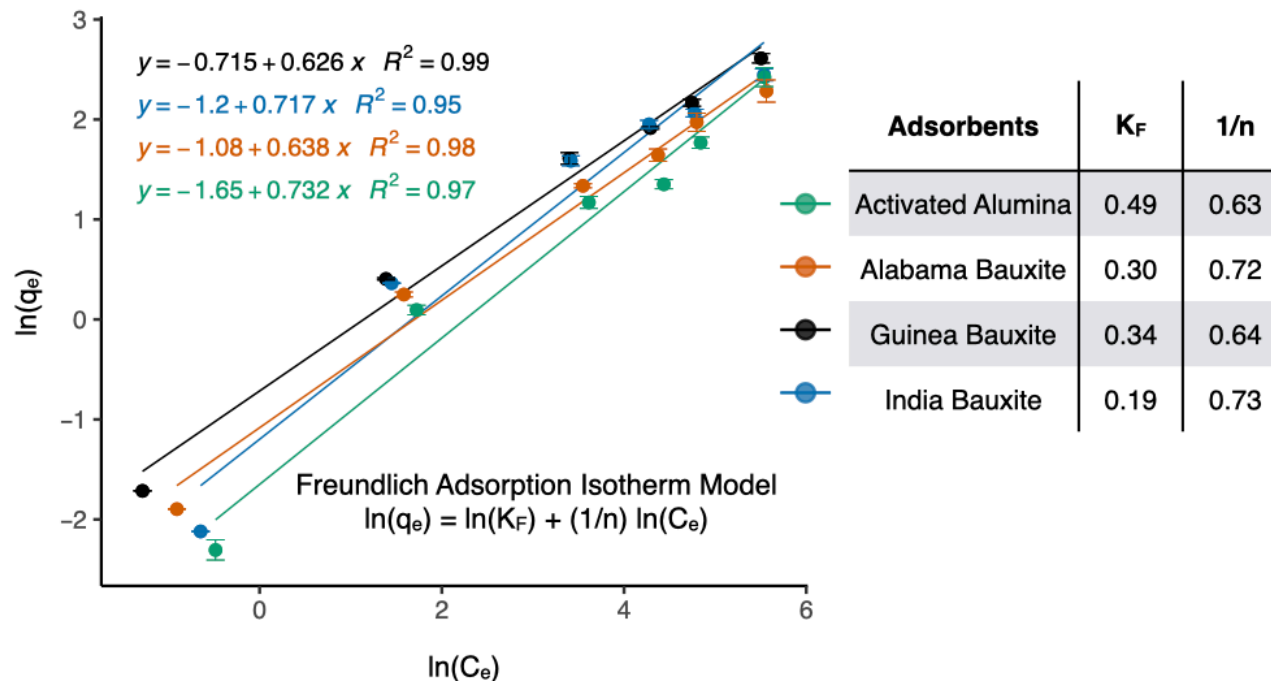


Fig. S8. Adsorption data of activated alumina and global bauxites (particle size **X**: 0.3-1.2mm) equilibrating with various initial fluoride concentrations ($C_o = 1 - 300 \text{ mg F}^- \text{ L}^{-1}$) in unaltered synthetic groundwater ($\text{pH}_o = 8.7$). The experimental data was best fit to an empirical Freundlich isotherm model (solid lines) and described by the parameters K_F (adsorption capacity) and $1/n$ (adsorption strength).

10. Filter Column Breakthrough by Number of Pore Volumes - Fig. S9

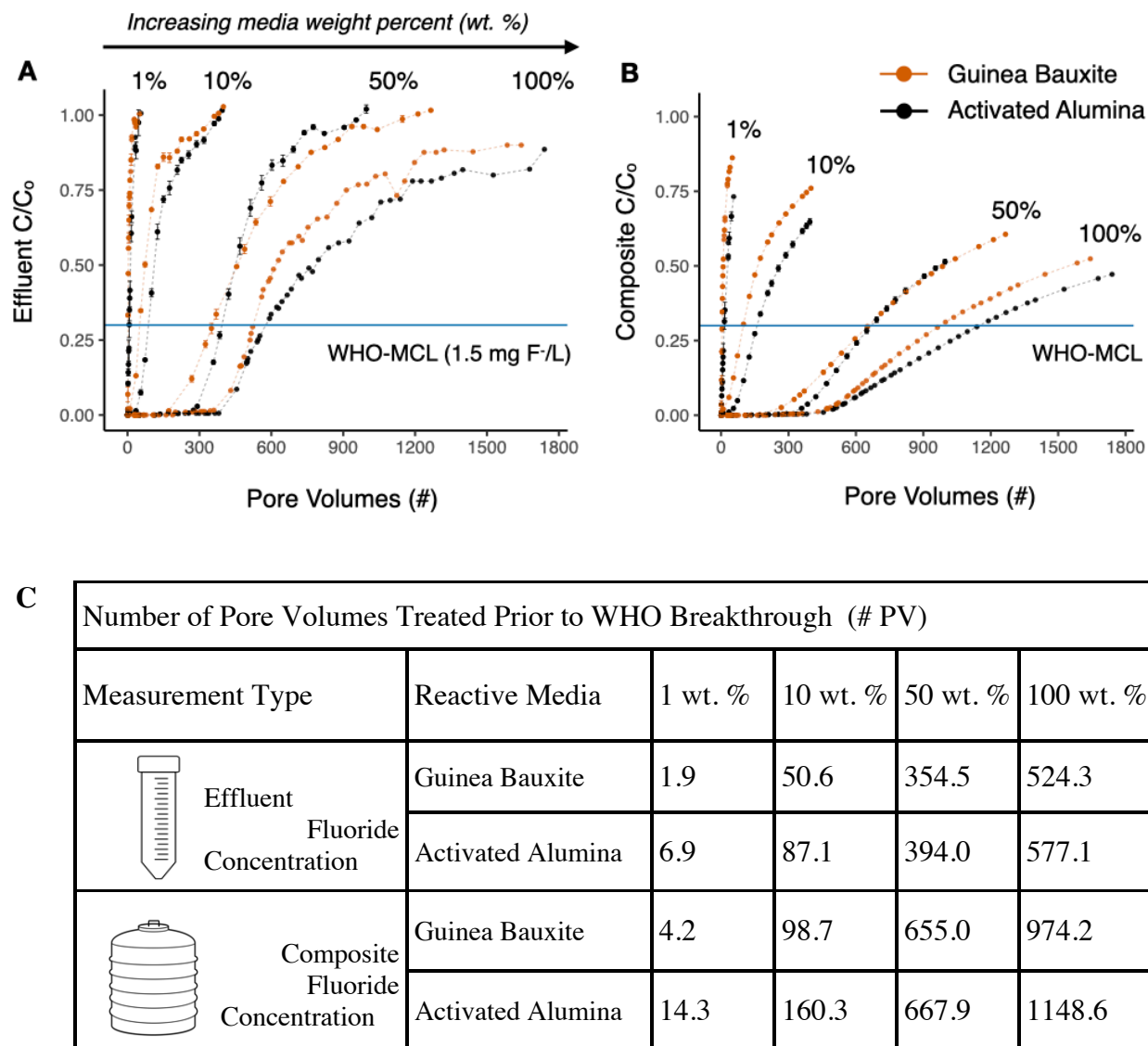


Fig. S9. Breakthrough of fluoride (in terms of number of pore volumes) in synthetic groundwater ($C_o = 5 \text{ mg F}^- \text{ L}^{-1}$; $\text{pH}_o = 8.7 \pm 0.2$) using columns packed with increasing weight percent (1, 10, 50, 100 wt. %) of activated alumina and Guinea bauxite. Panel (A) shows breakthrough in terms of effluent fluoride concentrations measured instantaneously and Panel (B) shows averaged composite fluoride concentrations. Panel (C) summarizes number of pore volumes treated prior to partial breakthrough for both concentration measurement types. The horizontal blue line in panels A and B represents the partial breakthrough limit, the World Health Organization's Maximum Contaminant Limit for fluoride in drinking water (WHO-MCL = $1.5 \text{ mg F}^- \text{ L}^{-1}$). Averages of fluoride concentration measurements taken from duplicate experiments are presented for the 1, 10, 50 wt. % columns, along with calculated standard deviations. The 100 wt. % column data represent single column studies.

11. Parameter Value Estimation for BDST Model - Fig. S10

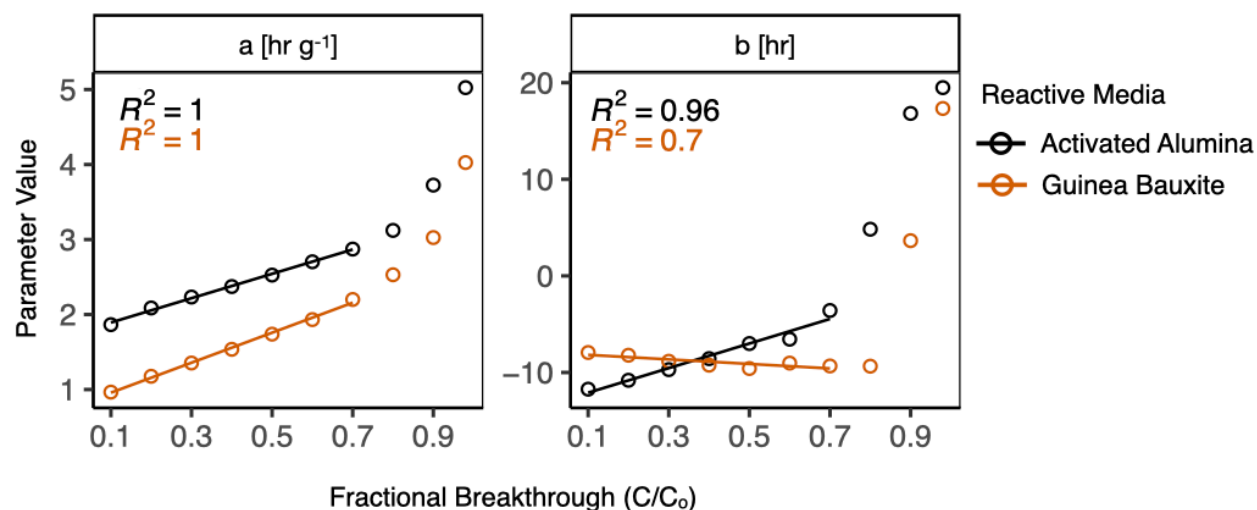


Fig. S10. Slope ‘a’ and intercept ‘b’ of the Bed Depth Service Time (BDST) model behave linearly as a function of fractional breakthrough C/C_0 , up to a breakthrough of approximately 0.7. Model parameter estimates (solid lines) were calculated based on experimental data (points) from column studies using 1, 10, and 50 wt. % of activated alumina and Guinea bauxite.

The BDST model parameter value scale linearly up to a fractional breakthrough (C/C_0) of 0.6 and 0.7 for Guinea bauxite and AA, while b scales linearly up to a fractional breakthrough of 0.5 and 0.6 for Guinea bauxite and AA. To determine scaling parameters for a large-scale system operating to a fractional breakthrough of 0.5, it is sufficient to experimentally determine parameters at a much lower breakthrough and extrapolate. In the case of our 100 wt.% columns, this shortcut would have reduced our experimental time by up to 35%, or approximately a week. Additional research is necessary to validate the use of the BDST model for predicting contaminant breakthrough at different influent concentrations and approach velocities.

12. Estimation of Time to Filter Media Saturation

One approach to estimate the time to media saturation (and frequency of column backwashing and media regeneration) is presented in studies characterizing adsorbent media used in stormwater treatment systems (Grebel et al., 2016; Hatt et al., 2009; Ray et al., 2019). Using the following parameters obtained from our lab-scale column study and making assumptions about the field-scale treatment system, we can calculate the time when activated alumina (AA) and Guinea bauxite (GB) reach saturation and need to be regenerated:

Lab Parameters & Field Assumptions:

The column breakthrough curves in **Fig 4** indicate that the fully packed (100 wt. %) columns of activated alumina ($M = 165 \text{ g}$; $\rho_{\text{bulk, AA}} = 1.031 \text{ kg L}^{-1}$) and Guinea bauxite ($M = 228 \text{ g}$; $\rho_{\text{bulk, GB}} = 1.425 \text{ kg L}^{-1}$) can respectively treat 58.3 L and 56.1 L of potable water, before the effluent water quality exceeds the WHO breakthrough limit ($1.5 \text{ mg F}^{-} \text{ L}^{-1}$). The following calculations assume that the adsorbent media will be used in an existing large-scale Kenyan water treatment facility described earlier in Section 3.5 ($Q = 1250 \text{ L hr}^{-1}$; $C_o = 5 \text{ mg F}^{-} \text{ L}^{-1}$; $H = 1.5 \text{ m}$; $D = 0.925 \text{ m}$; $V = 1008 \text{ L}$; $d_p = 0.75 \text{ mm}$). The flow rate Q reflects a $10,000 \text{ L day}^{-1}$ plant being operated for 8 hours daily to provide enough water for a small community (i.e., $3.65 \times 10^6 \text{ L yr}^{-1}$).

Calculation Steps:

- 1) Annual fluoride mass in field = influent fluoride concentration * volume of water treated by the large system:

$$5 \text{ mg F}^{-} \text{ L}^{-1} * 3.65 \times 10^6 \text{ L yr}^{-1} = 1.83 \times 10^7 \text{ mg F}^{-} \text{ yr}^{-1}$$

Adsorption density = fluoride mass removed in column operation / packed adsorbent mass:

$$\text{AA: } ((5 - 1.5 \text{ mg F}^{-} \text{ L}^{-1}) * 58.3 \text{ L}) / 165 \text{ g AA} = 1.20 \text{ mg F}^{-} \text{ g}^{-1}$$

$$\text{GB: } ((5 - 1.5 \text{ mg F}^{-} \text{ L}^{-1}) * 56.1 \text{ L}) / 228 \text{ g GB} = 0.86 \text{ mg F}^{-} \text{ g}^{-1}$$

- 2) Fluoride mass treated in field = Adsorption density * bulk packed bed density * empty field bed volume:

$$\text{AA: } 1.20 \text{ mg F}^{-} \text{ g}^{-1} * 1031 \text{ g L}^{-1} * 1008 \text{ L} = 1.29 \times 10^6 \text{ mg F}^{-}$$

$$\text{GB: } 0.86 \text{ mg F}^{-} \text{ g}^{-1} * 1425 \text{ g L}^{-1} * 1008 \text{ L} = 1.24 \times 10^6 \text{ mg F}^{-}$$

- 3) Media lifetime = annual fluoride load in the field / mass of fluoride treated in the field:

$$\text{AA: } 1.29 \times 10^6 \text{ mg F}^{-} / 1.83 \times 10^7 \text{ mg F}^{-} \text{ yr}^{-1} = 0.070 \text{ yr} = 25.7 \text{ days} = \mathbf{0.85 \text{ months}}$$

$$\text{GB: } 1.24 \times 10^6 \text{ mg F}^{-} / 1.83 \times 10^7 \text{ mg F}^{-} \text{ yr}^{-1} = 0.068 \text{ yr} = 24.7 \text{ days} = \mathbf{0.81 \text{ months}}$$

These calculations provide a first order estimate (and worst-case scenario) of regeneration frequency because they do not account for backwashing or other filter operation methods that can improve an adsorbent's lifetime. Furthermore, the calculations assume that all water produced by the column during the initial filtration stages is used to dilute composite drinking water once its quality begins to deteriorate. However, the output of multiple columns run in parallel and of columns run out of phase may be combined to maintain proper dilution as well as a constant yield of drinking water.

13. Fluoride Adsorption Kinetics Normalized by Particle Size - Fig. S11

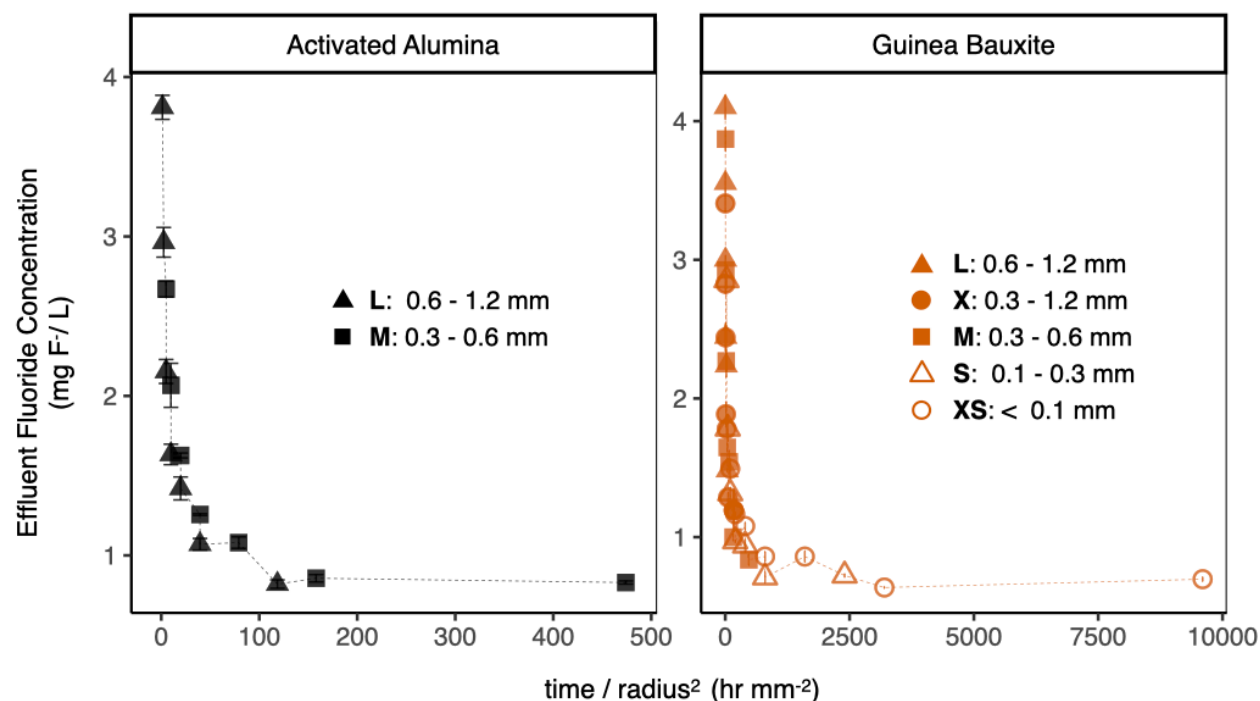


Fig. S11. Experimental fluoride adsorption kinetics data plotted as effluent fluoride concentration versus time normalized by the squared radius of each adsorbent media. The radii of each media's particle size ranges were approximated as the average between the upper and lower bound for activated alumina (**L**: 0.6-1.2 mm and **M**: 0.3-0.6 mm) and Guinea Bauxite (**L**: 0.6-1.2 mm, **X**: 0.3-1.2 mm, **M**: 0.3-0.6 mm, **S**: 0.1-0.3 mm, and **XS**: < 0.1 mm). Overlapping points representing various particle size ranges in the normalized kinetics curves suggest that the Rapid Small Scale Column Testing (RSSCT) diffusion coefficient, which describes movement of fluoride ions through interior pores in the adsorbent media, is independent of media particle size. Dotted lines connect raw experimental data points and do not represent a model fit.